

Cold Plasma Effect on Optical Properties of Polypyrrole Thin Films

Hadeer Kamel and Hamid H. Murbat

Department of Physics, College of Science for Women, University of Baghdad, 10071 Baghdad, Iraq

hadeer.ali1604@cs.w.uobaghdad.edu.iq, hamidmurbat@gmail.com

Keywords: Polypyrrole, FTIR, Cold plasma, Electrochemical, UV-Vis.

Abstract: Electrochemical deposition of polypyrrole (PPy) thin films was performed on indium tin oxide (ITO) glass substrates using potassium nitrate (KNO_3) as the supporting electrolyte. Extensive surface modifications of the conductive polymers were then performed by cold plasma treatment (using a DBD plasma device) at various time points (0, 5, 10, 15, and 20 minutes). Polypyrrole is a self-conducting polymer that undergoes radical structural and chemical changes in the presence of plasma. This work aimed to investigate the changes in polypyrrole (PPy) films using Fourier transform infrared (FTIR) spectroscopy, focusing on the use of oxygen-containing groups, changes in C=C and C-N vibrations, and UV-vis spectroscopy. Optical tests were also performed to measure the energy gap at different time points, in addition to the overall effect of cold plasma on the surface activity/conductivity of polypyrrole. These results indicate that plasma treatment is an effective post-treatment tool for improving the functional properties of electrochemically synthesized polypyrrole membranes and their potential applications in sensors, energy storage systems, and optoelectronics.

1 INTRODUCTION

Conductive polymers featuring double bonds have recently garnered considerable interest as sophisticated materials. Polypyrrole demonstrates superior performance in commercial applications owing to its excellent environmental stability, high conductivity, and relative simplicity of production in comparison to numerous other polymers. Polypyrrole is predominantly utilized in various domains, including biosensors [1], [2], sensors for gas [3], [4], the wiring [5], micro actuators [6], a solid capacitor that are electrolytic [7] functional films, packaging materials, electromagnetic shields, polymer battery packs, electrical appliances [8], electrochemical devices, and also capacitors [9], [10]. It exhibits swift oxidation and reduction, excellent biocompatibility [11], [12], and low weight [13]. Conductor polymers have been distinguished through their rapid doping and de-doping capabilities [14]-[18]. Polymers are produced using chemical and electrochemical polymerisation processes. Recent studies have demonstrated that plasma polymerisation is a significant technique for generating thin films of the conductive polymer polypyrrole (PPy) [19]-[25].

Plasma, defined as a near-neutral gas, is the fourth state of matter and accounts for more than 99% of the matter in the universe. There are more common states of matter, including solid, liquid, and gas. Plasma consists of positive and negative ions, electrons, and atoms. Plasma is classified according to its temperature into high-temperature plasma and low-temperature plasma [26]. On the other hand, plasma treatment is used to improve the surface of polymers. It does not alter the properties of the base material, but it does alter its electrical and chemical properties [27], [28]. Surface modification is often necessary to improve compatibility and functionality. We rely on Cold plasma treatment, a non-thermal method, and also use gases such as O_2 , N_2 , and Ar to add new functional groups and modify the polymer surface without significant degradation. Cold plasma simultaneously cleans the surface, removing weak surface areas, eliminating wettability, and improving contact angles [29]. The dielectric barrier discharge (DBD) method, one of the non-thermal plasma systems or designs, has received positive feedback from most studies due to its scalability and reliable plasma production. In recent years, research has increased on atmospheric DBD plasma. This type of plasma is known for its ability to modify surfaces and its low cost without affecting bulk properties [29].

This system will be used and relied upon for processing and exposing samples to cold plasma. In this study, we will investigate the effect of cold plasma on the optical properties of electrochemically produced polypyrrole (PPy) thin films. The films were exposed to cold plasma for a specified period before their changes were examined using different methodologies. Fourier transform infrared (FTIR) spectroscopy provides valuable insights into the structural changes of the PPy polymer by detecting changes in the vibrational patterns of chemical bonds. The purpose of FTIR analysis in this study is to focus on the plasma-treated chemical modifications in PPy polymer films. We also used ultraviolet-visible spectroscopy to study the optical properties and electronic changes of the polypyrrole films. This examination revealed that the cold plasma significantly affected the absorption behavior of PPy, leading to modifications in its optical absorption properties due to changes in the molecular structure or surface morphology. We also revealed an increase in the intensity of the bands that occurred during interactions between the polypyrrole and the plasma as a function of exposure time.

2 MATERIALS AND METHODS

2.1 Materials

The chemicals utilized for the electrochemical deposition of polypyrrole (PPy) films are pyrrole monomer C_4H_5N as the starting material and potassium nitrate KNO_3 as the secondary material. Indium tin oxide (ITO)-coated glass is required, and deionized and distilled water is used for pretreatment. The samples are subjected to cold plasma annealing using a DBD system. Analyses include Fourier transform infrared (FTIR) spectroscopy and UV-visible spectroscopy.

2.2 Experimental Methods

The reaction solution was prepared and electrochemically deposited. The polypyrrole membrane preparation process followed several steps. This was accomplished using 0.1 M pyrrole and 0.2 M potassium nitrate (KNO_3) as co-electrolytes. The molecular weights of each solution were determined

Where $M = \text{moles of pyrrole (67.09 g/mol)}$ and $101.1 \text{ g/mol} = \text{moles of potassium nitrate}$. Their masses were measured using a high-sensitivity balance and then determined. A volume of distilled or

deionized water was added to the determined masses, bringing the volume to 100 mL in a graduated cylinder. The 0.1 M pyrrole solution was then diluted to 0.07 M.

After dilution, the remaining volume was removed and diluted with distilled or deionized water to reach the final volume. 20 ml of pyrrole.

Add a drop of dilute pyrrole solution to a 0.2 M potassium nitrate solution, and the final solution is complete. To complete the final solution, add 6 liters of pyrrole and 6 liters of potassium nitrate.

We need indium tin oxide (ITO)-coated glass for the deposition process. The glass is cut into small squares, and the ITO pieces are soaked in an ethanol mixture for 10 minutes to ensure cleanliness. The pieces can then be rinsed with distilled water and dried using parchment paper. A digital voltmeter is used to determine the conductive side of the ITO glass by measuring the resistance of one of the other two surfaces. The zero side (low resistance) serves as the active electrode surface. Once the reaction solution is complete and the glass is prepared, the electrochemical deposition process begins. We place the reaction solution in a beaker and place two electrodes in it along with 12 liters of water. The anode material is indium tin oxide (ITO) glass, and the cathode is nickel. We connect the electrodes to a 4-volt DC power supply and leave them there for 5 minutes. A thin layer of indium tin oxide glass begins to deposit on the conductive side of the polypyrrole, resulting in a thin layer of polypyrrole on the glass only. After the specified time has elapsed, the electrodes are disconnected from the power supply, and the indium tin oxide glass is thoroughly rinsed with distilled and plain water. The samples were prepared in the same manner five times.

After the electrochemical deposition was complete, one of the five samples was not exposed to plasma (i.e., the control). The remaining samples were exposed to cold plasma for various durations, which we will describe. This is accomplished using a DBD system for generating cold plasma, which we will rely on in this study. This system consists of two titanium-coated stainless-steel electrodes with a quartz barrier between them. The system operates using high-voltage alternating current (HVAC). The applied voltage was 25 kV, the distance between the top electrode of the DBD and the surface was 2 mA, the thickness of the polypyrrole film was 1 mm, and the voltage frequency was 28 kHz. The system mainly consists of high-voltage electrodes. Cold plasma was obtained by ionizing atmospheric air and applying it to the sample for different exposure times (5, 10, 15, and 20 min). The electrode was separated from the

ITO glass surface by a distance of 2 mm to discharge the plasma generation. After the five samples were fully plasma treated, several analytical tests were performed to analyze their optical properties. Fourier transform infrared (FTIR) spectroscopy was studied, while the optical absorption behavior was studied using UV-visible spectroscopy.

3 RESULTS AND DISCUSSION

3.1 UV-Vis Spectroscopy

The optical properties are essential for evaluating the optical behavior of prepared thin films and assessing their potential applications. These properties are influenced by several factors such as irradiation process, the adding of incorporated nanoparticles, the nature of the polymer, and the preparation technique [30]. The UV-vis spectra of PPy and irradiated PPy samples at different time (5, 10, 15 and 20 min) are presented in Figure 1. The obtained results revealed there are four main bands for all samples at (345 nm, 437 nm, 581 nm and 762 nm), the characteristic band centered at (345 nm) is as a result to electronic transitions from the valence band to the anti-bonding polaronic states [31]. The absorption band centered at (437 nm) can be attributed to the high energy polaronic transitions [32]. While the absorption band centered at (581 nm) attributed to the electronic transitions involving the bipolaron band or interband transitions between the valence band and the bipolaron/antibonding polaronic states [33]-[35].

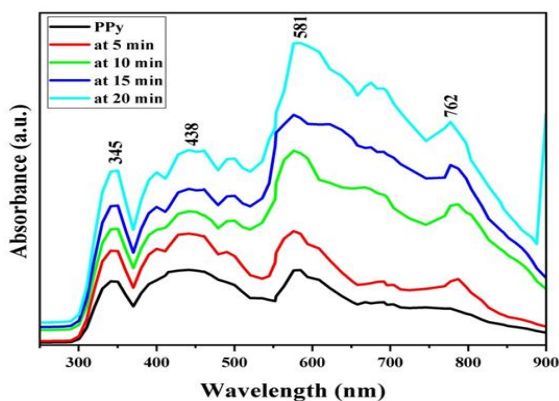


Figure 1: The UV-vis spectra of PPy and irradiated PPy at different time (5, 10, 15 and 20 min).

From Figure 1, the obtained results of irradiated PPy samples at different time (5, 10, 15 and 20 min) demonstrate the increase of the absorbance intensities

with the plasma exposure time, this can be explained as the plasma irradiation can be attributed to multiple mechanisms. Plasma treatment can introduce surface functional groups and increase surface roughness, thereby enhancing light trapping and absorption. Additionally, plasma exposure can lead to oxidation and doping level changes, which modify the π - π transitions in the conjugated polymer chains, resulting in enhanced optical absorption. Structural modifications such as increased conjugation length or formation of localized energy states also contribute to greater absorbance intensity. These changes collectively improve the optical activity of material, particularly in the UV visible region [36]-[38].

The fourth absorption band centered at (762 nm) appeared after the plasma irradiation process of the PPy and the intensity became higher with the increase of the exposure time, which attributed to electronic transitions involving bipolaronic states, plasma irradiation enhances oxidation and doping levels within the polymer chains, resulting in increased bipolaron formation. These modifications shift the absorbance toward the near-infrared region due to transitions from the valence band to the bipolaronic energy levels, as well as changes in the conjugation length and electronic structure of the polymer backbone [39].

The results indicated that the plasma irradiation significantly influences the absorbance behavior of polypyrrole, leading to modifications in its optical absorption characteristics due to changes in molecular structure, surface morphology, or doping levels. The increase of the band's intensity revealed the interactions between the PPy and the plasma as a function of the exposure time.

Figure 2 and Table 1 show the E_g band gap energy values for the PPy material. This band gap was determined by plotting $(\alpha h\nu)^2$ versus $(h\nu)$. The band gap value for the material not exposed to cold plasma (control) exhibits the first semiconducting behavior of this sample at an E_g value of 3.29 eV, obtained after plotting $(\alpha h\nu)^2$ as a result and calculating. This is a relatively high value, indicating that a large amount of electron energy is required to induce the transition between the conduction and valence bands. This is likely due to the presence of few doping states in this sample, as the deposition of electrochemical materials is unchanged. The band gap energy in the PPy polymer plot exposed to cold plasma for 5 minutes was found to be approximately 3.2 eV. This increase indicates a decrease in the lengths of the conjugated bonds of the polymer and the occurrence of oxidation, leading to a decrease in the number of damage sites and an increase in the band gap through

the redistribution of the electronic structure of the material and an improvement in its dielectric properties. The curve indicated that as the plasma exposure time increased to 10 minutes, the energy gap increased significantly to approximately 2.6 eV. This suggests that the polymer structure underwent more significant changes during the plasma treatment, with more conjugated bonds being broken and new oxygen groups forming on the surface. This resulted in reduced activation and structural disorder. Consequently, the polymer exhibited weaker light absorption and isolation behavior compared to the sample treated after 5 minutes. This demonstrates that the optical gap is higher in the cold plasma treatment than in the cold plasma treatment, due to the alteration of the PPy polymer's electronic structure. This value indicates that the effect of 15 minutes of cold plasma treatment on the energy gap was negligible. This is

attributed to the fact that the plasma altered the electronic and surface structure of the material, removing some protons from electron-donor groups and increasing the periodicity of the polymer chains, resulting in an energy gap of approximately 3.1 eV for the Tauc curve of the polypyrrole (PPy) sample exposed to cold plasma for 20 minutes. This means that plasma exposure caused saturation of the oxide layer and a further increase in structural defects, resulting in a slight decrease in the gap compared to the sample treated for 10 minutes. This is attributed to the fact that high perturbation causes the evolution of local energy conditions within the gap. However, it can be definitively concluded that initially, the longer the plasma treatment time, the larger the gap, which then stabilizes or decreases slightly with longer treatment times due to partial damage to the conjugate bond and surface defects.

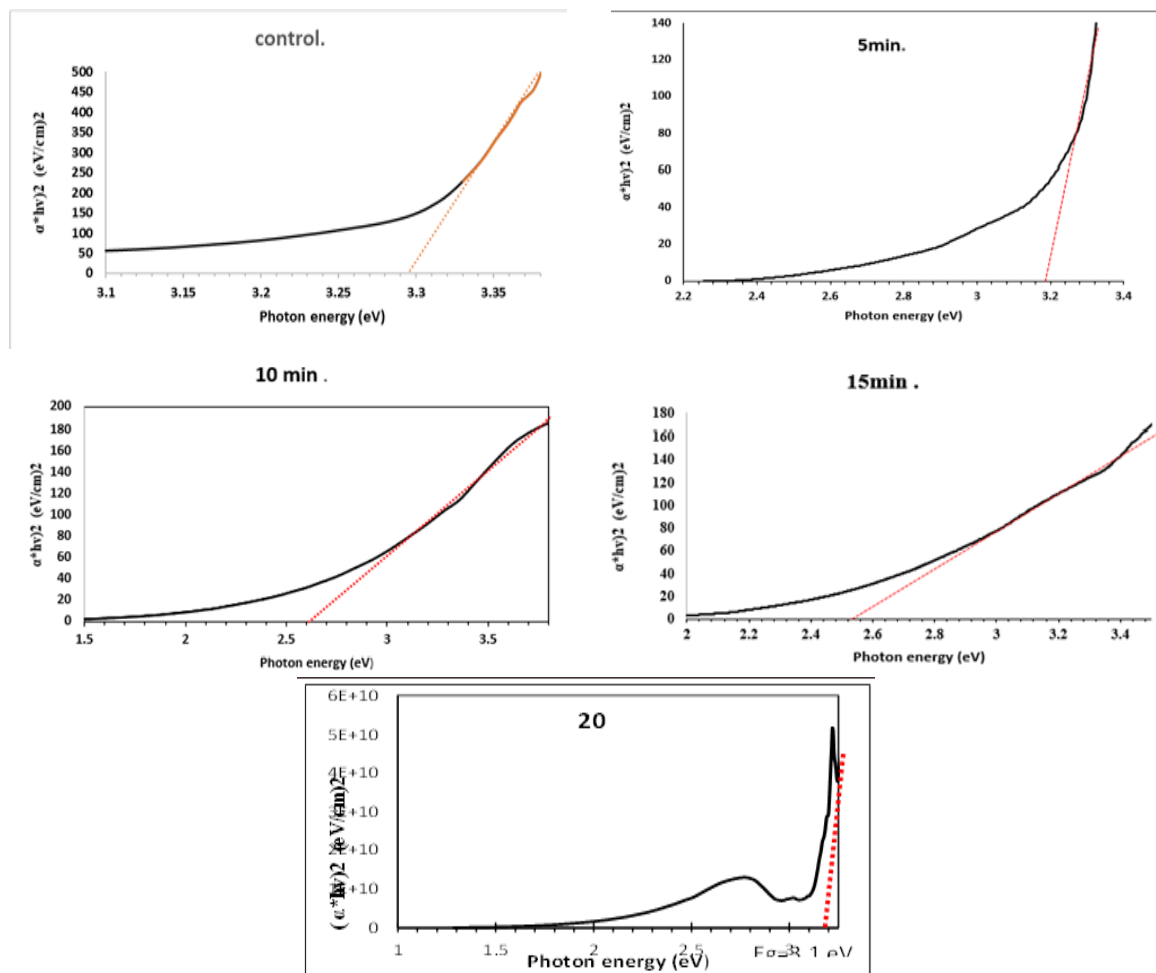


Figure 2: Tauc plots of $(\alpha h\nu)^2$ versus photon energy $(h\nu)$ for PPy thin films: pure PPy PPy after cold plasma irradiation for (5,10,15,20) min used to determine the optical band gap.

Table 1: The energy gap values for PPy material unexposed and exposed to cold plasma at different times (5, 10, 15, 20) minutes.

Sample	Exposure time (min)	Eg (eV)
PPy-0	0	3.29
PPy-5	5	3.2
PPy-10	10	2.6
PPy-15	15	2.4
PPy-20	20	3.1

3.2 Fourier Transform Infrared Spectroscopy (FTIR)

Fourier transform infrared (FTIR) spectroscopy results of polypyrrole films exposed to cold plasma for different time periods (0, 5, 10, 15 and 20 minutes). The aim was to determine how the films interact with each other. Such spectra signal the fact that various peaks or bands of various functional groups are present in the PPy structure which is evident in the Figure 3.

These peaks will make us identify the peaks or bands. The wide band at 3421 cm^{-1} has signified the N-H stretching vibration in the polypyrrole. The absorption peak of O-H stretching vibration, dissolved in hydrogen bonds within the polymer chain, appears in the peak at 3425 cm^{-1} [40]

We find an absorption band of the C-H bond stretching vibration of the aliphatic compound at 2922 cm^{-1} and 2924 cm^{-1} . Such peaks are correspondent with findings of the researcher [41]

The band at $2800\text{-}2900\text{ cm}^{-1}$ is attributed to the stretching vibration of C-H and band at 1381 cm^{-1} to the stretching vibration of N-H in the ring. This complies with the peaks reported by the researcher. The C=O bond vibration with a wavenumber of 1632 cm^{-1} shows that the treated film contained carbonyl groups. The band of $1250\text{-}1340\text{ cm}^{-1}$ is a typical C-N bond stretching aromatic rings or primary amines characteristic band of PPy structure. These are at 1463 cm^{-1} , 1465 cm^{-1} and 1460 cm^{-1} representing C-C, C-H and C-N bending that are the characteristic vibrational bands of conventional PPy aromatic rings [41, 42] This conforms to the findings of the researcher. Another study has reported this pyrrole polymerization to happen at 796 cm^{-1} [43] A band at 720 cm^{-1} corresponds to out of plane stretching the C-H bond, commonly used as a detector of aromaticity.

The plasma-treated samples, shown in Figure 2, also exhibit a curve in which the characteristic absorption peaks shifted somewhat to a shorter wavelength region (higher wavenumber) after cold plasma treatment. This blue shift is attributed to the

increased vibrational energy of these functional groups.

FTIR spectra show some of the main absorption bands of polypyrrole (PPy) and their slight changes after plasma treatment. The peaks at frequencies of 720 and 796 cm^{-1} are attributed to out-of-plane C-H bending vibrations generated by the pyrrole ring, while the peaks observed between frequencies of 1250 and 1340 cm^{-1} , which also appear at 1381 cm^{-1} , are attributed to C-N bond stretching, in addition to the C-C bending vibration. The signals at frequencies of 1465 cm^{-1} and 1632 cm^{-1} are attributed to C=C and C=O stretching, respectively. The broad absorption band at frequencies of $2800\text{-}2900\text{ cm}^{-1}$ and the peak at 2924 cm^{-1} arise from C-H stretching and aliphatic bending, respectively, while the peaks at frequencies around 3421 (N-H stretching) or 3425 cm^{-1} (O-H stretching) are attributed to hydrogen-bonded groups. The peak shift toward a shorter wavelength is attributed to plasma-induced changes, such as oxidation, crosslinking, or penetration of polar functional groups on the polymer surface. These effects lead to stronger chemical bonds and improved.

The peak shift toward a shorter wavelength is attributed to plasma effects (oxidation, crosslinking, or penetration of polar functional groups) on the polymer surface. These effects directly affect the strongest chemical bonds, promoting what we call increased collective behavior.

Interactions between PPy chains. Therefore, we interpret the observed blue shift as evidence of increased bond energy and a change in the chemical environment of the PPy chains as a result of cold plasma treatment, resulting in a more cohesive and energetically stable polymer network.

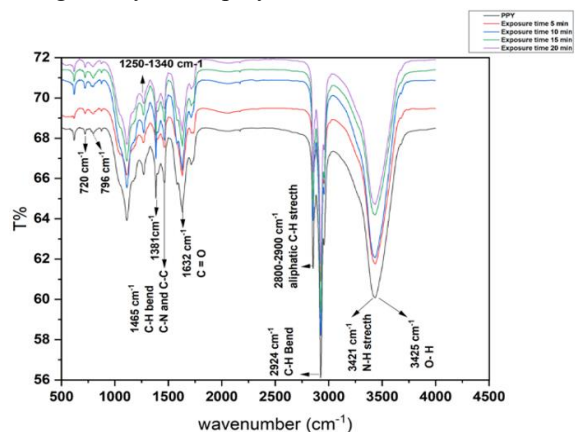


Figure 3: FTIR analysis of PPy and PPy exposed to cold plasma at different times (5, 10, 15 and 20 min).

4 CONCLUSIONS

After cold plasma treatment of polypyrrole films and surface chemical synthesis, Fourier transform infrared (FTIR) analysis revealed the appearance of carbonyl and hydroxyl groups (C_N, C_C), a decrease in vibrations, and a broad band at 3421 cm^{-1} , representing the N-H bond vibration. This indicates structural changes in the molecular structure of polypyrrole resulting from cold plasma exposure. The plasma gas and exposure duration significantly affect the oxidation level and functionalization. However, plasma enhances the functional group density and surface reductivity. Excessive exposure may lead to decreased electrical conductivity due to chain cleavage. UV-Vis spectroscopy results also indicate that cold plasma irradiation significantly affects the absorption behavior of polypyrrole, leading to modifications in photoresistance properties due to changes in molecular structure, surface shape, or doping levels. The increased band intensity revealed interactions between polypyrrole and plasma as a function of exposure time. The band gap energy (E_g) of unexposed PPy was found to be 3.29 eV, a relatively high peak indicating a high electron energy requirement to induce the transition between the absorption and valence bands. In contrast, the band gap energy of PPy exposed to cold plasma for 5 minutes was approximately 3.2 eV. This increase suggests a decrease in the conjugate lengths of the polymer and the occurrence of oxidation, leading to a reduction in the number of damage sites and an increase in the band gap through the redistribution of the material's electronic structure. We conclude that the longer the plasma treatment duration, the greater the band gap, which stabilizes or slightly deviates with longer treatment periods due to cleavage and increased structural disorder. Therefore, optimal plasma conditions are essential for improving the properties of polypyrrole to meet the needs of sensors, energy devices, and biomedical coatings.

REFERENCES

- [1] J. C. Vidal, E. García, and J. R. Castillo, "In situ preparation of a cholesterol biosensor: Entrapment of cholesterol oxidase in an overoxidized polypyrrole film electrodeposited in a flow system: Determination of total cholesterol in serum," *Analytica Chimica Acta*, vol. 385, no. 1-3, pp. 213-222, 1999.
- [2] T. Campbell, A. Hodgson, and G. Wallace, "Incorporation of erythrocytes into polypyrrole to form the basis of a biosensor to screen for rhesus (D) blood groups and rhesus (D) antibodies," *Electroanalysis: An International Journal Devoted to Fundamental and Practical Aspects of Electroanalysis*, vol. 11, no. 4, pp. 215-222, 1999.
- [3] N. Kemp et al., "Temperature-dependent conductivity of conducting polymers exposed to gases," *Synthetic Metals*, vol. 101, no. 1-3, pp. 434-435, 1999.
- [4] D. Kincal, A. Kumar, A. D. Child, and J. R. Reynolds, "Conductivity switching in polypyrrole-coated textile fabrics as gas sensors," *Synthetic Metals*, vol. 92, no. 1, pp. 53-56, 1998.
- [5] C. Jérôme, D. Labaye, I. Bodart, and R. Jérôme, "Electrosynthesis of polyacrylic/polypyrrole composites: Formation of polypyrrole wires," *Synthetic Metals*, vol. 101, no. 1-3, pp. 3-4, 1999.
- [6] E. Smela, "Microfabrication of PPy microactuators and other conjugated polymer devices," *Journal of Micromechanics and Microengineering*, vol. 9, no. 1, p. 1, 1999.
- [7] C. MA, P. SG, G. PR, M. RN, S. Shashwati, and P. VB, "Synthesis and characterization of polypyrrole (PPy) thin films," *Soft Nanoscience Letters*, vol. 2011, 2011.
- [8] G. Wallace, G. Spinks, and P. Teasdale, *Conductive Electroactive Polymers*. New York: Technomic, 1997.
- [9] S. Takagi, S. Makuta, A. Veamatahau, Y. Otsuka, and Y. Tachibana, "Organic/inorganic hybrid electrochromic devices based on photoelectrochemically formed polypyrrole/TiO₂ nanohybrid films," *Journal of Materials Chemistry*, vol. 22, no. 41, pp. 22181-22189, 2012.
- [10] Y. Shi et al., "Nanostructured conductive polypyrrole hydrogels as high-performance, flexible supercapacitor electrodes," *Journal of Materials Chemistry A*, vol. 2, no. 17, pp. 6086-6091, 2014.
- [11] R.-J. Lee, R. Temmer, T. Tamm, A. Aabloo, and R. Kiefer, "Renewable antioxidant properties of sursensible chitosan-polypyrrole composites," *Reactive and Functional Polymers*, vol. 73, no. 8, pp. 1072-1077, 2013.
- [12] J. Jang and J. H. Oh, "Fabrication of a highly transparent conductive thin film from polypyrrole/poly (methyl methacrylate) core/shell nanospheres," *Advanced Functional Materials*, vol. 15, no. 3, pp. 494-502, 2005.
- [13] J. Guo et al., "Magnetite-polypyrrole metacomposites: Dielectric properties and magnetoresistance behavior," *The Journal of Physical Chemistry C*, vol. 117, no. 19, pp. 10191-10202, 2013.
- [14] R. Hasanov and S. Bilgiç, "Monolayer and bilayer conducting polymer coatings for corrosion protection of steel in 1 M H₂SO₄ solution," *Progress in Organic Coatings*, vol. 64, no. 4, pp. 435-445, 2009.
- [15] B. Zeybek, N. Ö. Pekmez, and E. Kılıç, "Electrochemical synthesis of bilayer coatings of poly (N-methylaniline) and polypyrrole on mild steel and their corrosion protection performances," *Electrochimica Acta*, vol. 56, no. 25, pp. 9277-9286, 2011.

- [16] D. E. Tallman, G. Spinks, A. Dominis, and G. G. Wallace, "Electroactive conducting polymers for corrosion control: Part 1. General introduction and a review of non-ferrous metals," *Journal of Solid State Electrochemistry*, vol. 6, no. 2, pp. 73-84, 2002.
- [17] C. B. Breslin, A. M. Fenelon, and K. G. Conroy, "Surface engineering: Corrosion protection using conducting polymers," *Materials & Design*, vol. 26, no. 3, pp. 233-237, 2005.
- [18] M. González and S. Saidman, "Electrodeposition of polypyrrole on 316L stainless steel for corrosion prevention," *Corrosion Science*, vol. 53, no. 1, pp. 276-282, 2011.
- [19] M. Silverstein and I. Visoly-Fisher, "Plasma polymerized thiophene: Molecular structure and electrical properties," *Polymer*, vol. 43, no. 1, pp. 11-20, 2002.
- [20] M. B. Inoue, M. A. Bruck, M. Carducci, Q. Fernando, and M. Inoue, "A new bis (ethylenedithio) tetrathiafulvalene chloride:(BEDT-TTF)₂Cl·3H₂O," *Synthetic Metals*, vol. 38, no. 3, pp. 353-361, 1990.
- [21] C.-T. Kou and T.-R. Liou, "Characterization of metal-oxide-semiconductor field-effect transistor (MOSFET) for polypyrrole and poly (N-alkylpyrrole)s prepared by electrochemical synthesis," *Synthetic Metals*, vol. 82, no. 3, pp. 167-173, 1996.
- [22] M. Omastová, S. Kosina, J. Pionteck, A. Janke, and J. Pavlinec, "Electrical properties and stability of polypyrrole containing conducting polymer composites," *Synthetic Metals*, vol. 81, no. 1, pp. 49-57, 1996.
- [23] A. Bozkurt, U. Akbulut, and L. Toppare, "Conducting polymer composites of polypyrrole and polyindene," *Synthetic Metals*, vol. 82, no. 1, pp. 41-46, 1996.
- [24] Y.-I. Su, J. Wang, and H.-z. Liu, "FTIR spectroscopic study on effects of temperature and polymer composition on the structural properties of PEO-PPO-PEO block copolymer micelles," *Langmuir*, vol. 18, no. 14, pp. 5370-5374, 2002.
- [25] S. Hotta, M. Soga, and N. Sonoda, "Novel organosynthetic routes to polythiophene and its derivatives," *Synthetic Metals*, vol. 26, no. 3, pp. 267-279, 1988.
- [26] V. Nehra and A. Kumar, *Atmospheric Non-Thermal Plasma Sources*, 2008.
- [27] A. Sikora et al., "Surface modification of PMMA polymer and its composites with PC61BM fullerene derivative using an atmospheric pressure microwave argon plasma sheet," *Scientific Reports*, vol. 11, no. 1, p. 9270, 2021.
- [28] N. Yasoob A, H. H. Murbat, and K. J. Khaleel, "The influence of cold atmospheric pressure plasma on TSH and thyroid hormones in male rats," in *AIP Conference Proceedings*, 2020, vol. 2213, no. 1, p. 020015.
- [29] N. Q. Mohammed and H. H. Murbat, "Treatment of epoxy surface by DBD cold atmospheric," *Ibn Al-Haitham Journal for Pure and Applied Sciences*, vol. 37, no. 2, pp. 203-214, 2024.
- [30] K. K. Ahmed et al., "A brief review on optical properties of polymer composites: Insights into light-matter interaction from classical to quantum transport point of view," *Results in Physics*, vol. 56, p. 107239, 2024.
- [31] D. N. Huyen, N. T. Tung, T. D. Vinh, and N. D. Thien, "Synergistic effects in the gas sensitivity of polypyrrole/single wall carbon nanotube composites," *Sensors*, vol. 12, no. 6, pp. 7965-7974, 2012.
- [32] J. Arjomandi and R. Holze, "Spectroelectrochemistry of conducting polypyrrole and poly (pyrrole-cyclodextrin) prepared in aqueous and nonaqueous solvents," *Journal of Solid State Electrochemistry*, vol. 11, no. 8, pp. 1093-1100, 2007.
- [33] A. G. MacDiarmid and A. J. Epstein, "Polyanilines: A novel class of conducting polymers," *Faraday Discussions of the Chemical Society*, vol. 88, pp. 317-332, 1989.
- [34] J. R. Pawar, M. E. Dudhamal, K. K. Rathod, and R. A. Joshi, "Synthesis and characterization of polypyrrole thin films," *International Journal of Science and Research Archive*, vol. 14, no. 1, pp. 902-907, 2025.
- [35] M. Warren and J. D. Madden, "A structural, electronic and electrochemical study of polypyrrole as a function of oxidation state," *Synthetic Metals*, vol. 156, no. 9-10, pp. 724-730, 2006.
- [36] E. Kang, K. Neoh, K. Tan, and F. Loh, "Surface modified and functionalized polyaniline and polypyrrole films," *Synthetic Metals*, vol. 84, no. 1-3, pp. 59-60, 1997.
- [37] G. E. Martín-Pat et al., "Effect of different exposure times on physicochemical, mechanical and biological properties of PGS scaffolds treated with plasma of iodine-doped polypyrrole," *Journal of Biomaterials Applications*, vol. 35, no. 4-5, pp. 485-499, 2020.
- [38] H. Katouah and N. M. El-Metwaly, "Plasma treatment toward electrically conductive and superhydrophobic cotton fibers by in situ preparation of polypyrrole and silver nanoparticles," *Reactive and Functional Polymers*, vol. 159, p. 104810, 2021.
- [39] M. Santos, A. Brolo, and E. Girotto, "Study of polaron and bipolaron states in polypyrrole by in situ Raman spectroelectrochemistry," *Electrochimica Acta*, vol. 52, no. 20, pp. 6141-6145, 2007.
- [40] S. Sayyah, F. Mohamed, and M. Shaban, "Electropolymerization of (ortho methoxy phenol-copolyrrole) and characterization of the obtained film," *Applied Chemistry*, vol. 7, no. 1, p. 2278, 2014.
- [41] M. F. Ghadim, A. Imani, and G. Farzi, "Synthesis of PPy-silver nanocomposites via in situ oxidative polymerization," *Journal of Nanostructure in Chemistry*, vol. 4, no. 2, p. 101, 2014.
- [42] A. Castro-Beltran, C. G. Alvarado-Beltran, J. F. Lara-Sanchez, W. de la Cruz, F. F. Castillon-Barraza, and R. Cruz-Silva, "Electrochemical deposition of polypyrrole in the presence of silanes as adhesion promoters," *Polymers*, vol. 15, no. 10, p. 2354, 2023.
- [43] N. M. Rosas-Laverde, A. Pruna, and D. Busquets-Mataix, "Improving electrochemical properties of polypyrrole coatings by graphene oxide and carbon nanotubes," *Nanomaterials*, vol. 10, no. 3, p. 507, 2020.